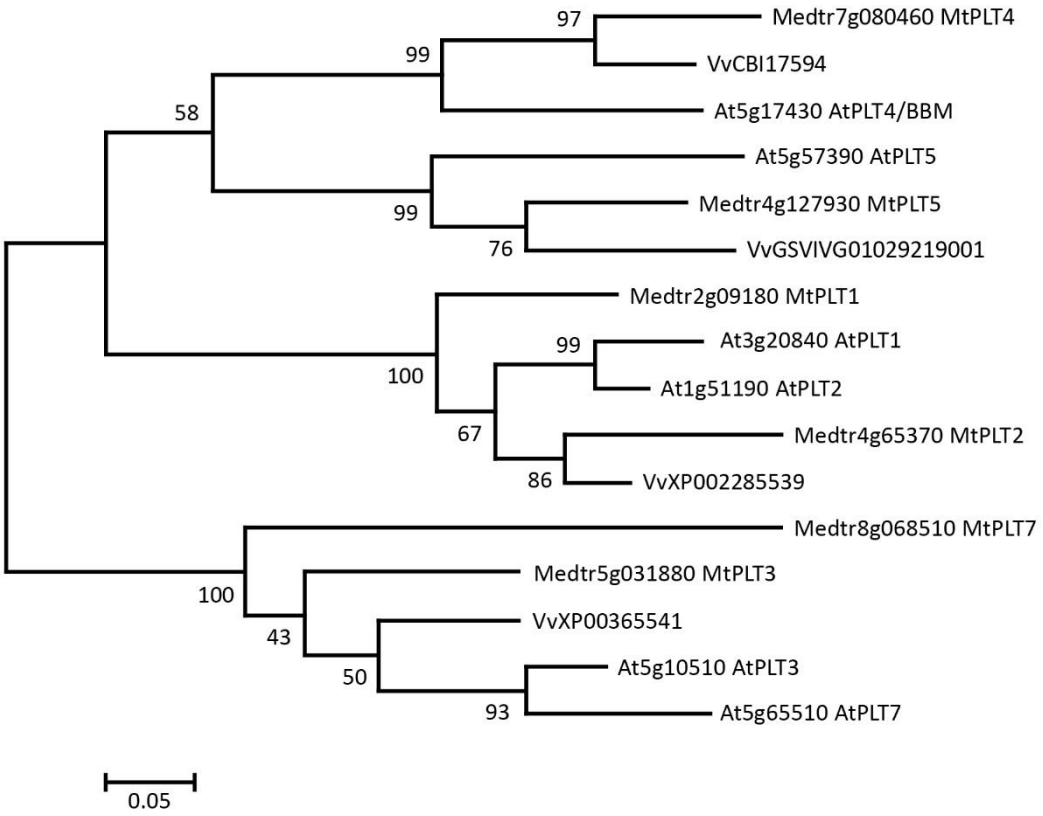

Fig. S1. Orthology between Arabidopsis and Medicago *PLT* genes.
Maximum likelihood phylogenetic tree of PLETHORA proteins from Arabidopsis, Medicago and *Vitis venifera* (as outgroup). The Arabidopsis protein names are according to Prasad et al 2011 , resolving the tree into four clades, the PLT1/2, PLT3/7, PLT4 and PLT5 clades respectively. The Medicago protein sequences were obtained after reciprocal BLAST of Arabidopsis protein sequences through TBLASTN on Mt4.0 v1CDS (http://blast.jcvi.org/er-blast/index.cgi?project=mtbe) followed by BLASTX against the Arabidopsis protein database of the nucleotide sequences of the retrieved Medicago proteins. The Vitis proteins were retrieved by BLASTP of Arabidopsis proteins. The Vitis genome contains one gene copy for each of the four clades. The midpoint rooted tree was constructed with MEGA version 5.1 (Tamura et al., 2011), using default parameters (bootstrap values of 500 replicates).

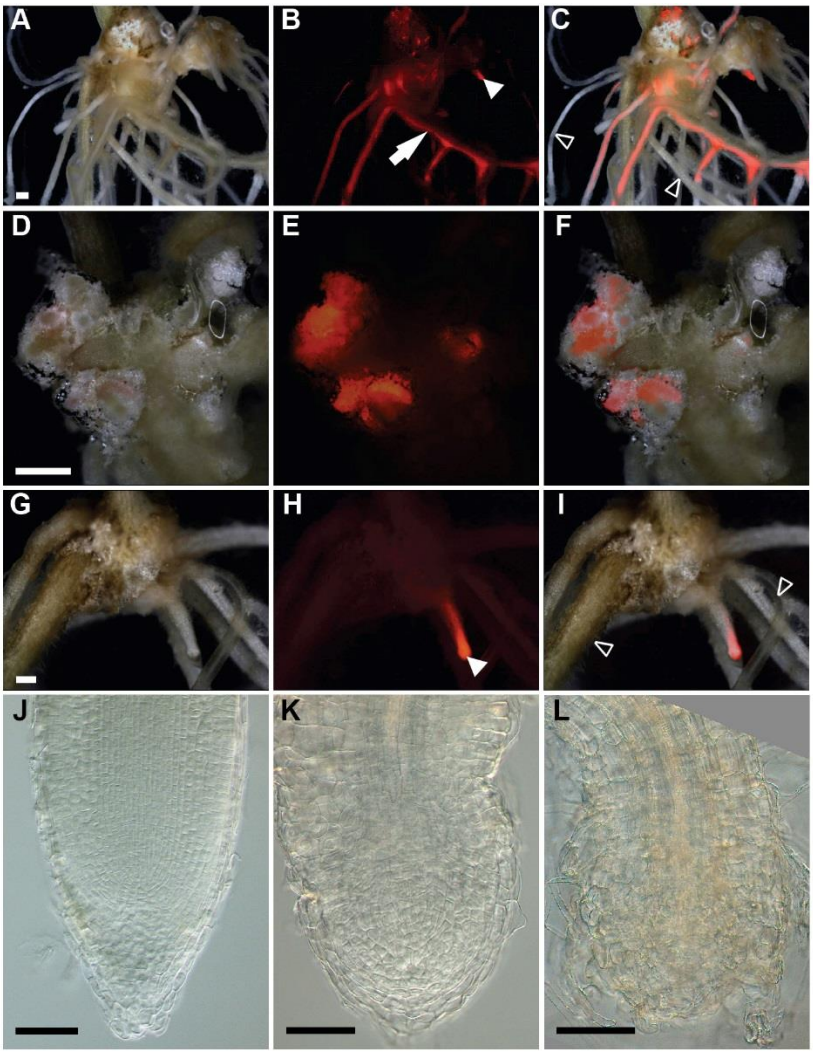

Fig. S2. Transgenic hairy root formation requires *MtPLT1-4* gene expression
(A-I) Vector control transgenic calli readily generate hairy roots (A-C, arrow, arrowhead), in contrast to *35S::MtPLTi* transgenic calli (D-I). (J-L) Occasionally from some *35S::MtPLTi* calli short transgenic roots appear (H; arrowhead), compared to long roots formed on vector control transgenic calli (B, arrow). When compared to vector control roots (J), the meristem of these short roots is severely affected or absent soon after emergence (K, L; note the presence of root hairs as a marker for differentiation). (M) Average number of short and long roots formed on transgenic calli of *35S::MtPLT1i,2i*, *35S::MtPLT3i,4i*, *35S::MtPLTi* and empty vector control transgenic roots, shows that *35S::MtPLTi* leads to a strong reduction in roots formed from transgenic calli.
(A, D, G) Bright field; (B, E, H) dsRed filter; (C, F, I) overlay. (J-L) Bright field with Nomarski objectives.

Bars 240µm (A-I) and 75µm (J-L).

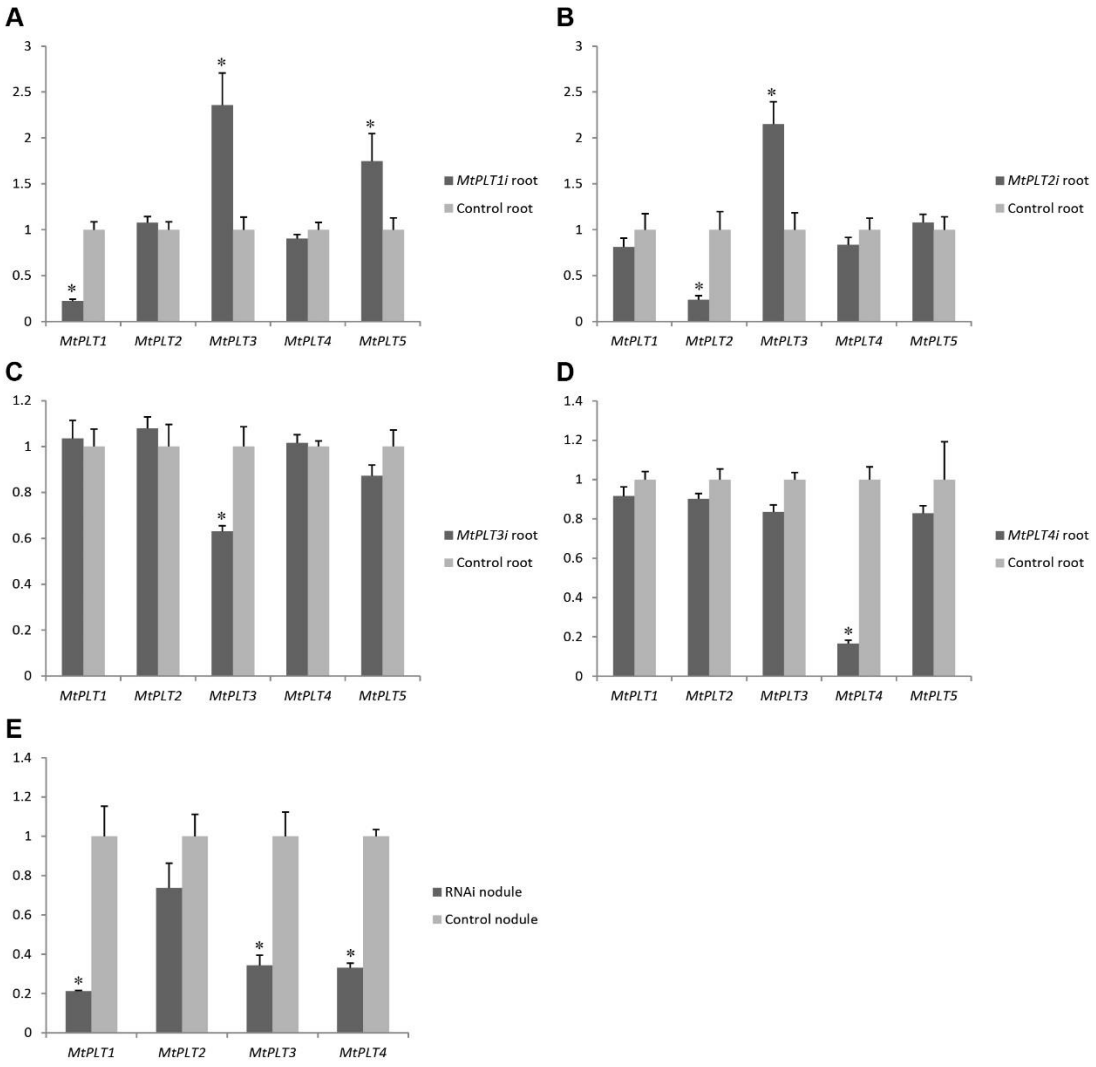

Fig. S3. *MtPLT* expression levels in single *35S::MtPLT* RNAi root and nodules.
(A-E) Relative *MtPLT* expression in single *35S::MtPLT* RNAi roots (A-D, gray bar) and 15 d old nodules (E, gray bar) compared to their expression in control roots and nodules (black bar), respectively. Relative expression levels were determined by qPCR and normalized to 1 in control plants for each *MtPLT* gene using *MtACTIN-2*. Shown graphs are the means ± s.e.m. of two biological repeats. Significance of expression reduction of tested *MtPLT* gene in RNAi versus expression of this gene in control samples is indicated by * as $P<0.05$ in Student t test.

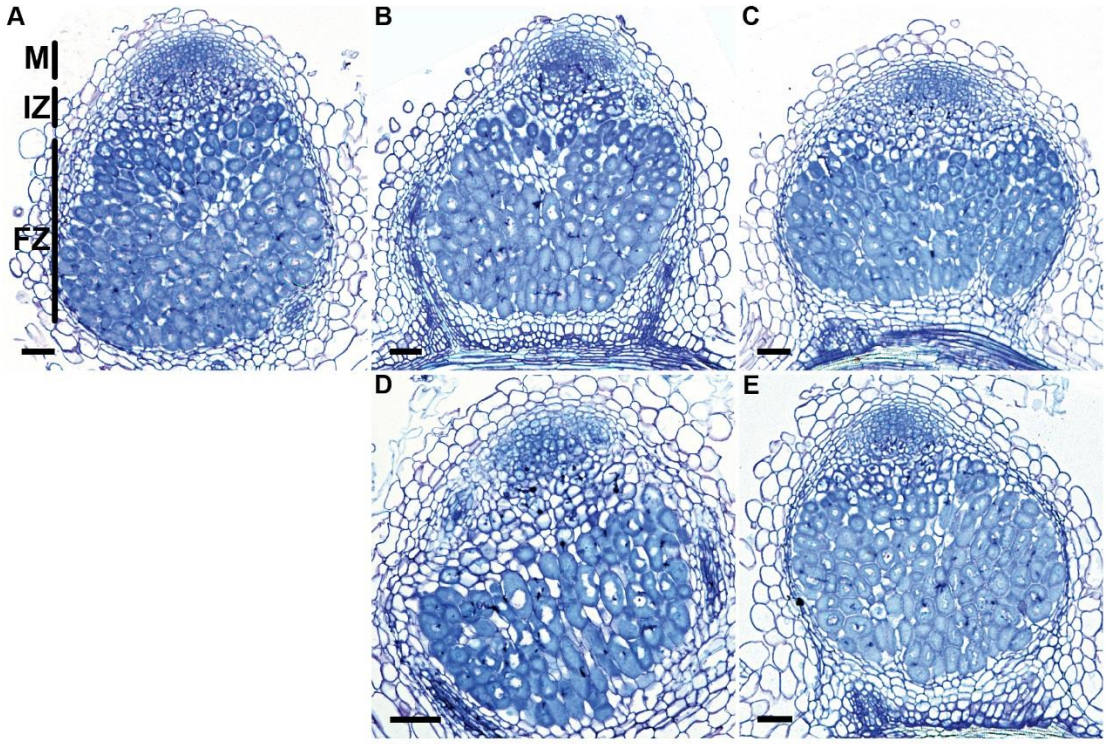

Fig. S4. Longitudinal sections of representative single *MtPLT* RNAi nodules.
(A) Median section through a control nodule. (B-E) representative median section through *35S::MtPLT1i* (B), *35S::MtPLT2i* (C), *35S::MtPLT3i* (D) and *35S::MtPLT4i* (E) nodule. All nodules were sampled 15 d after inoculation. For statistics on cell layers per zone see Table S3. M, meristem; IZ, infection zone; FZ, fixation zone.

Bars 75μm.

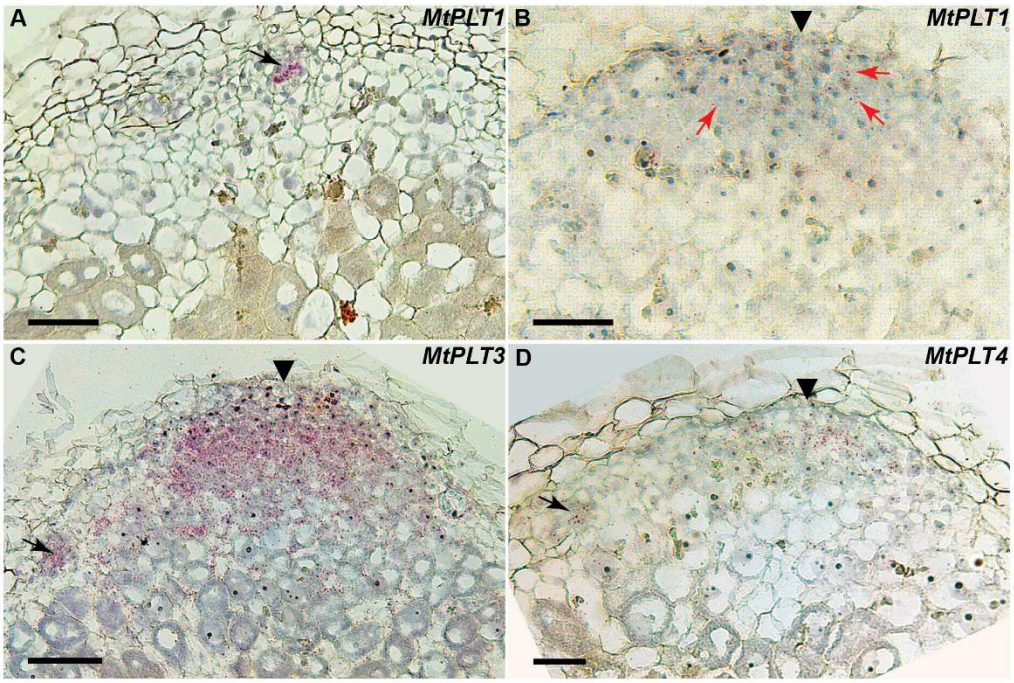

Fig. S5. RNA *In situ* hybrization of *MtPLT1*, *MtPLT3* and *MtPLT4* in nodules.
To validate the *pMtPLT::GUS* patterns, we conducted ISH on sections of 15day old nodules with gene specific probes of (A, B) *MtPLT1*, (C) *MtPLT3* and (D) *MtPLT4* visualized as pink grains. (A, B) Note the high expression level of *MtPLT1* in NVM (A, arrow) and the very low level in the NCM (B, arrowhead). (C) *MtPLT3* expression is in the NM and in the infection zone, while (D) *MtPLT4* expression is restricted to NM. The *MtPLT2* ISH expression pattern described (Roux et al., 2014) is in agreement with the *pMtPLT2::GUS* expression pattern (Fig. 6 G-I) and for *MtPLT1,3,4* genes the ISH pattern is similar to the *pMtPLT1,3,4::GUS* pattern (Fig. 6 G-L), respectively. This indicates that the *pMtPLT::GUS* patterns are reflecting *MtPLT* transcripts. Arrows point to NVM, arrowheads to NCM. Red arrows in B point to individual grains indicating the low expression of *MtPLT1* in the NCM.

Bars 75µm.

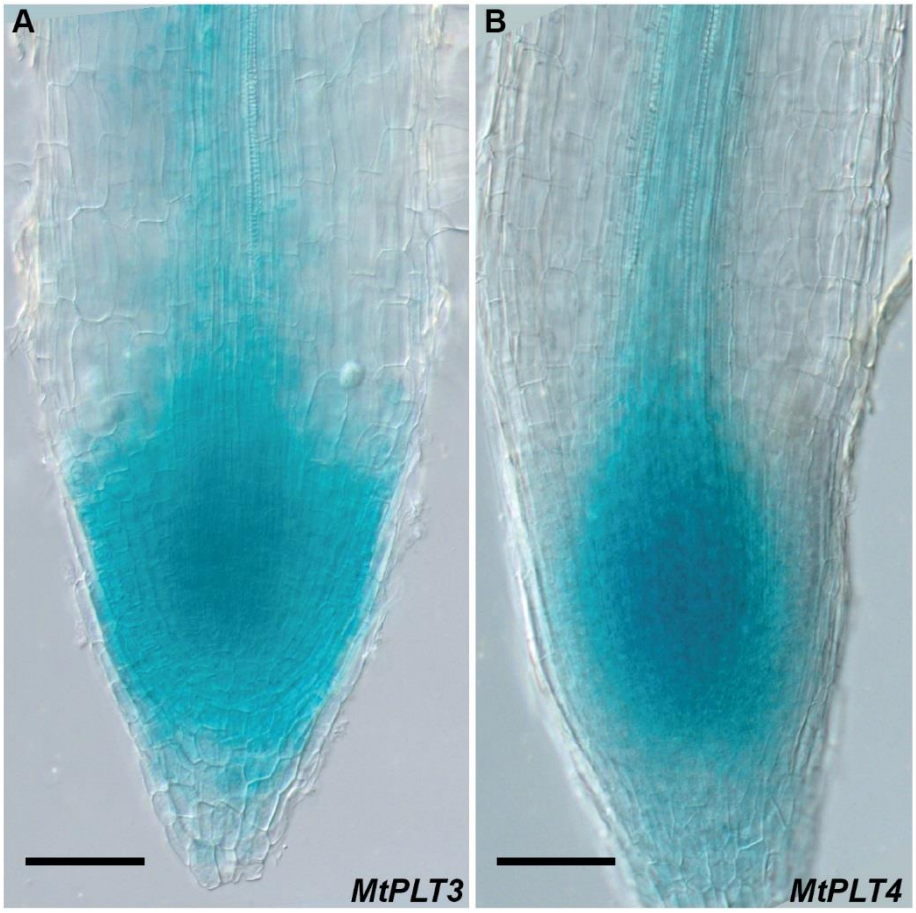

Fig. S6. *MtPLT3::GUS* and *MtPLT4::GUS* expression patterns in the root.
(A) *MtPLT3::GUS* and (B) *MtPLT4::GUS* expression patterns extend into the root vascular tissue.

Bars 75µm.

Table S1. Root formation and growth upon *35S::MtPLT* RNAi transformation

SR, short roots (<3 cm); LR, long roots (>3 cm).

transgene	Calli	Roots	SR	LR	Roots/callus
35S::EV	18	62	4	58	3.5
35S::MtPLT1i,2i	20	22	13	9	~1
35S::MtPLT3i,4i	27	78	12	66	~3
35S::MtPLTi	16	4	4	0	0.25
pENOD12::EV	16	41	2	39	2.5
pENOD12::MtPLTi	16	32	1	31	2

Table S2. Nodule formation on *35S::MtPLT* RNAi transgenic roots.

Number of nodules/root in two independent experiments involving at least 15 roots per experiment. Data was collected 15 days after inoculation. EV is empty vector.

	Number of analysed roots	Nodules/root
35S::EV	70	3.2±0.2
35S::MtPLT1i	46	3.1±0.1
35S::MtPLT2i	32	3.3±0.2
35S::MtPLT3i	42	3.1±0.4
35S::MtPLT4i	49	3.4±0.2

Table S3. Quantification of nodule histology upon single *35S::MtPLT* RNAi

Analyses of 20 control nodules shows that the meristem consists of 4-6 cell-layers and the central tissue of 16-19 cell layers distributed over 6-7 cell-layers in the infection zone and 10-12 cell layers in the fixation zone. Compared to control nodules, all zones of single *35S::MtPLT* RNAi nodules consist of a number of cell layers that is within the variation observed in the control. Data was collected in two biological replicas and 15 days after inoculation.

	Meristem	Infection zone	Fixation zone	Nodule number
control	4-6	6-7	10-12	20
MtPLT1i	4-6	6-8	10-14	19
MtPLT2i	4-7	5-7	9-10	17
MtPLT3i	4-5	6-8	8-10	20
MtPLT4i	4-7	7-9	8-12	17

Table S4. Nodule formation on *ENOD12::MtPLT* RNAi transgenic hairy roots in three independent experiments

C represents nodules formed on control transgenic hairy roots generated using the empty vector only expressing the DsRED selection marker. N is the average number of nodules per root (18 roots per construct per experiment). The percentage of reduced number of nodules (%) on *MtPLT* RNAi roots is significant at P< 0.05 for *MtPLT1i,2i* and *MtPLT3i,4i* (Mann Whitney test) or at P<0.01 for *MtPLTi* (Mann Whitney test)

C (N)	*MtPLT1i,2i* (N)	%	*MtPLT3i,4i* (N)	%	*MtPLTi* (N)	%
5.8	3.1	47	3	49	1	83
6.2	3.0	52	3.3	47	1.1	83
6.0	3.1	49	2.9	52	1.5	75

Table S5. Primers used in this study

promoters	
MtpPLT1F	caccgacttgacggtgaaggtt
MtpPLT1R	gcacaacctgcatctaaaaagtttact
MtpPLT2F	caccatccaaacacacccttagtc
MtpPLT2R	gagggaatgaaagccagttattgttc
MtpPLT4F	cacctctcaaatagaatttacctccaac
MtpPLT4R	gaaagaaaaaaaaagacaaagagagatcgg
MtpPLT3F	caccttgcactcccctcctctcaaag
MtpPLT3R	caaagtctttgaacagaaacaacgg
MtpWOX5F	cacccaaccaagccttatcatagtat
MtpWOX5R	gctctcttccatatttcaattctaga
single *MtPLTi*	
MtPLT2F	cacctgaacacacacaacagcaatgaagttcc
MtPLT2R	gaagttctttgtccaaatgtctctg
MtPLT 1F	caccccttgatgaatagtagtcacaactc
MtPLT 1R	tcttgttacaccacgatatattgatg
MtPLT 4F	caccatcatcatcaacaacacttccc
MtPLT 4R	cctttaatctcactctcacc
MtPLT 3F	caccagcttcctcttcagttg
MtPLT 3R	cactgctactaccaacttc
MtPLT 3R2	cacccactgctactaccaacttc
double *MtPLTi*	
MtPLT 1com2R	gttgtgtgtgttcagccttgttacaccacg
MtPLT 2com1F	cgtggtgtaacaaggctgaacacacacaacag
MtPLT 4com3R	caactgaagagcatcatcaacaac
MtPLT 3com4F	gttgttgatgatgctcttcagttg
Quadruple *MtPLTi*	
12-43F	gggaagtgttgttgagaatagtagtcacaactc
43-12R	gagttgtgactactattctcaacaacacttccc
MtPLT 3R2	cacccactgctactaccaacttc
qPCR primers	
qMtPLT4F	tcacgaggtgcatccatttaccga
qMtPLT4R	acatcatatgcctctgctgcctct
qMtPLT1F2	ggaacttttggtaccgaggaa
qMtPLT1R2	tttgcagcacctcctcctat
qMtPLT2R	gcaatggttgaggttgttca
qMtPLT2F2	tcgagaaaacgcgaagaaat
qMtPLT3R	gttgctgctgctgctgttag
qMtPLT3F	tgacgtggaagcgataatga
qMtACT2F	cagatgtggatctccaagggtga
qMtACT2R	tgactgaaatatggcacaagactgaga
qMtPLT5F	cagtgataatccccacaatgc
qMtPLT5R	aagaaaatattggcgttgcg
qMtPLT7F	agaggcatacgaccttgcag
qMtPLT7R	ggaaggttttaagcgttttgc

Table S6. Strategy to obtain *MtPLT* DNA fragments for cloning into RNAi vectors.

Input fragment	First PCR primers	Second PCR primers	Final fragment
MtPLT1	MtPLT1F+Mt PLT1com2R	MtPLT1F+MtPLT2R	MtPLT1-MtPLT2
MtPLT2	MtPLT2com1F+MtPLT2R		
MtPLT3	MtPLT3com4F+MtPLT3R	MtPLT4F+ MtPLT3R	MtPLT3-MtPLT4
MtPLT4	plt4F+plt4com3R		
MtPLT1-MtPLT2	12-34F+MtPLT2R	MtPLT3R2+ MtPLT2R	MtPLT3-MtPLT4-MtPLT1-MtPLT2
MtPLT4-MtPLT3	MtPLT3R2+34-12R		